Green Chemistry

Microbial electrochemical treatment of biorefinery black liquor and resource recovery

Journal:	*Green Chemistry*
Manuscript ID	GC-ART-09-2018-002909.R2
Article Type:	Paper
Date Submitted by the Author:	30-Nov-2018
Complete List of Authors:	Chen, Xi; Princeton University Katahira, Rui; National renewable Energy Laboratory, Ge, Zheng; University of Colorado Boulder, Civil Environmental Engineering Lu, Lu; Princeton University, Civil and Environmental Engineering Hou, Dianxun; University of Colorado Boulder, Peterson, Darren; National Renewable Energy Laboratory, National Bioenergy Center Tucker, Melvin; National Renewable Energy Laboratory, (2) National Bioenergy Center Chen, Xiaowen; National Renewable Energy Lab, national bioenergy center Ren, Zhiyong; Princeton University, Civil and Environmental Engineering

Green Chemistry

ARTICLE

Microbial electrochemical treatment of biorefinery black liquor and resource recovery

Received 00th January 20xx,
Accepted 00th January 20xx

DOI: 10.1039/x0xx00000x

www.rsc.org/

Xi Chen[a,b], Katahira Rui[c], Zheng Ge[b], Lu Lu[a,b], Dianxun Hou[b], Darren Peterson[c], Melvin Tucker[c], Xiaowen Chen[c*], Zhiyong Jason Ren[a,b*]

Biorefineries valorize waste biomass to biofuels and bioproducts, but the associated wastewater treatment is costly and energy intensive. This study demonstrates that not only recalcitrant black liquor generated from biorefineries can be treated using microbial electrochemical process, value-added materials including lignin, chemicals, and H_2 can be separated to enable resource recovery. Lab scale microbial biomass recovery cell (MBRC) was developed to treat actual black liquor from the deacetylation and mechanical refining (DMR) process, and results show that 60.1-73.8% of organics, 52.0-54.6% of salts, and 30.8-49.5% of lignin were removed using different operational modes. Moreover, by utilizing the unique pH gradient generated between the different reactor chambers, tailored recoveries of lignin, chemicals, and H_2 were realized for the first time. The recoveries of lignin and salts were up to 61.2±2.7% and 92.2±1.6%, respectively. Ion transfer and organic transformation were further analyzed to understand the reaction mechanisms and improve system performance.

Introduction

Biorefineries convert waste biomass into value-added biofuels and bioproducts[1], but biomass waste treatment and utilization has been a major technical challenge and cost burden[2]. Biomass pretreatment enables selective fractionation and solubilization of the lignocellulosic biomass for subsequent enzymatic hydrolysis for biofuel production[2], but it generates a highly concentrated liquid waste stream from deacetylation called black liquor (BL)[3]. Black liquor contains various aromatic compounds and other toxic contaminants so it requires complex treatment processes[4]. Current commercial scale black liquor treatment used in Kraft pulping process involves evaporation and combustion by firstly concentrating the solid components followed by burning off the lignin and other organic matters and recovering sodium salts[5]. However, combustion of lignin limits biomass carbon utilization efficiency and leads to air pollutions and greenhouse gas emissions, but more importantly the many valuable components in black liquor such as acetate, lignin fragments, dissolved oligomeric hemicellulose, sugar degradation acids, and organic extractives, are underutilized[4].

Deacetylation and mechanical refining (DMR) pretreatment recently emerged as a promising biomass pretreatment process due to its high yields, reliability, and capability of lignin utilization[6, 7]. DMR uses dilute alkali such as NaOH to perform deacetylation under mild conditions, and it generates similar black liquor waste but more dilute with lower concentration of Na^+, K^+, and other ions. Because of this nature of DMR black liquor, concentrating the liquid stream for combustion is not feasible due to the high energy demand and low efficiency, but the spent ions are also too dilute (<10 g/L) to be cost effectively recovered by conventional Kraft process[8]. Traditional anaerobic digestion can degrade and convert black liquor organic matters to biogas, but the low value of biogas is hard to justify the treatment and energy collection, and the spent sodium salts accumulate in digestion biosolids[9]. When such biosolids are used in land application they will cause soil hardening and loss of crop productivity[10].

In this context, new processes are needed to not only treat black liquor wastes but also allow the recovery of value-added chemicals and products. In this study, we developed a new microbial electrochemical process tailored for black liquor resource recovery. We used the unique features of microbial electrochemistry to biologically degrade waste organics and convert the chemical energy into electrical potential, which is then used *in situ* for driving salt migration and recovery to enable a path to self-driven separation. More attractively, the pH gradients generated in different chambers of the reactor enable both lignin precipitation and separation as well as energy and salt recovery. The microbial electrochemical technology has been used to treat a variety of real wastewaters including the highly concentrated and recalcitrant waste streams from hydrothermal liquefaction, biorefining, and landfill leachate[11-15], and renewable energy and resources including electricity, H_2, nutrients, and salts have been recovered during the process[16-21].

[a.] *Department of Civil and Environmental Engineering and The Andlinger Center for Energy and the Environment, Princeton University, Princeton, NJ 08544 USA.*
[b.] *Department of Civil, Environmental, and Architectural Engineering, University of Colorado Boulder, Boulder, CO 80309 USA*
[c.] *National Bioenergy Center, National Renewable Energy Laboratory, 15013 Denver West Parkway, Golden, USA*
**Corresponding authors:*
Chen: Xiaowen.Chen@nrel.gov; Ren: zjren@princeton.edu
† Electronic Supplementary Information (ESI) available: [details of any supplementary information available should be included here]. See DOI: 10.1039/x0xx00000x

Table 1. Major composition of the raw concentrated DMR black liquor.

Substance	Content
Lignin	14.5~20.1 g/L
Xylan (oligomer)	5.9~8.6 g/L
Arabinan (oligomer)	4.6~4.9 g/L
Galactan (oligomer)	1.6~2.5 g/L
Glucan (oligomer)	1.8~2.3 g/L
Acetic acid	14.3~23.8 g/L
Lactic acid	6.9~8.3 g/L
Propionic acid	1.3~1.8 g/L
COD	88~97 g/L
pH	7.3~7.5
Conductivity	40~42 mS/cm
Na^+	11.1~11.7 g/L
K^+	1.6~2.5 g/L
Ca^{2+}	2.1~2.5 g/L
Mg^{2+}	0.6~0.8 g/L
SO_4^{2-}	0.2~0.5 g/L
PO_4^{3-}	0.6~0.9 g/L

Some microbial electrochemical processes can be self-driven by the electrical potential generated from organic removal and therefore demonstrated a promising closed-loop approach for energy efficient resource recovery[19, 22-24]. This study is the first that uses microbial electrochemistry to treat black liquor, the more important contribution lies in the direct utilization of the pH gradient for tailored lignin, salt, and H_2 recoveries, because such pH fluctuation has been previously considered a drawback of microbial electrochemical systems[25]. In this study, we developed and investigated the performance of the microbial biomass recovery cell (MBRC) for concurrent black liquor treatment and resource recovery, and we deciphered the removal and recovery mechanisms of the different chemicals in different reactor units and chambers.

2 Experimental section

2.1 Black liquor feedstock

Concentrated DMR black liquor samples were obtained from the Integrated Biorefinery Research Facility at the National Renewable Energy Lab (NREL, CO, United States) using corn stover (harvested in 2009 Hurley, South Dakota, US) as the biomass. The corn stover was firstly hammer milled and further knife milled to fit the rejection screen size (~19 mm)[8]. More detailed procedure on the black liquor generation using the DMR process can be found in our previous study[8]. Table 1 shows the main properties of the raw concentrated black liquor, which was obtained by repeated recycling of the black liquor generated during DMR operation[7, 8]. The main composition of the concentrated black liquor includes lignin, oligomer sugars, organic acids, and inorganic salts. The chemical oxygen demand (COD) concentration was 88~97 g/L, pH (neutralized) was 7.3~7.5, and the conductivity was 40~42 mS/cm.

2.2 Reactor construction and operation

To simulate the actual black liquor condition and investigate its treatability using microbial electrochemistry, preliminary testing was performed in two-chamber microbial electrolysis cells (MECs). Each reactor was equipped with a 20 cm x 10 cm x 1cm anode chamber with carbon felt anode and a same sized cathode chamber with NiFe nickel foam cathode[26]. The concentrated feedstock was diluted by 5, 10 and 20 times using deionized water, respectively. Each sample was mixed with anaerobic sludge (10:1 in volume) as the anode inoculum. A 50 mM phosphate buffer solution was used as the catholyte for the start-up of the bioanode. An external voltage of 1.0 V was applied to facilitate H_2 evolution on the cathode[27]. Electrical current and COD removal were measured for 30 days (Fig S1), and based on the comparative results, the 5-time dilution was used as the feedstock in the main experiments due to the stable current output and the fastest COD removal.

MBRC reactors were assembled by inserting a stacked membrane module in between the anode and cathode chambers. Each membrane module contained 3 pairs of ion exchange membranes

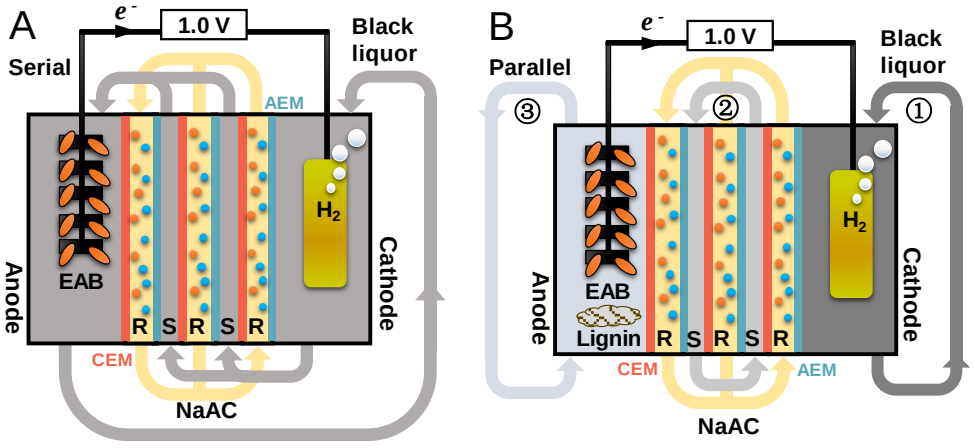

Figure 1. Schematic of the (A) serial-loop and (B) parallel-loop operations of the MBRC reactors. Red dots represent cations, while blue dots represent anions. EAB: electrochemical active bacteria; CEM: cation exchange membrane; AEM: anion exchange membrane; R: recovery chamber; S: separation chamber; ①: Cathode treatment; ②: Separation and recovery; ③: Anode treatment.

(Fig. 1). The cation exchange membranes (CEM, 1.8 mol/kg, Shanghua, China) and anion exchange membranes (AEM, 2.0 mol/kg, Shanghua, China) were alternately located in the stacked membrane module to form 3 recovery chambers and 2 separation chambers[24, 28]. The anode or cathode chamber was 1 cm in width, and each recovery and separation chambers were 0.5 cm wide. For ion recovery from the black liquor, deionized water was used as the recovery solution to collect the recovered ion species.

Fig. 1 also depicts the two operational modes used for black liquor treatment: the serial-loop mode and parallel-loop mode. In serial-loop operation, 600 mL black liquor was circulated sequentially from the cathode chamber to the separation chambers and then to the anode chamber for 144 hours (Fig. 1A). In parallel-loop operation, each chamber (cathode, separation, and anode) was individually circulated with separate black liquor feedstock (200 mL) (Fig. 1B, Fig. S2). After every 48-h operation, each bottle of black liquor was switched into the next downstream chamber, i.e. the effluent of the cathode to the separation chambers, and the effluent of separation chambers to the anode chamber. The outlet of the anode chamber was the final effluent of the whole parallel-loop MBRC operation. To compare the performance of the serial-loop, the parallel-loop mode was also operated as a 144-hour cycle, which consisted of three 48-h stages. During each cycle, the total volume of treated black liquor was 600 mL. For both the serial- and parallel-loop modes, the recovery solutions were renewed every 144 hours.

2.3 Analyses and calculations

The voltage (*U*, mV) across a 10 Ω external resistance (*R*, Ω) was recorded every 30 min by a data acquisition system (2700, Keithley Instruments, OH, USA) to calculate the current ($I=U/R$, mA)[29]. All water samples were filtrated using 0.45 μm nylon filter membranes before analyses. COD was measured using the standard HACH spectrophotometric method. The conductivity and pH were acquired using a conductivity meter and a pH meter, respectively. Hydrogen gas produced from the cathode was quantified using a gas chromatograph (Model 8610C, SRI Instruments). Main ions including Na^+, K^+, Ca^{2+}, Mg^{2+}, PO_4^{3-} and SO_4^{2-} were measured by ion chromatography (ICS-1100, DIONEX, USA). Acetate, lactate, propionate, and oligosaccharides were determined using NREL Laboratory Analysis Procedure (LAP No. NREL/TP-510-42627). Aromatic compounds were analysed using high-performance liquid chromatography (HPLC, Agilent 1100/1200). The column used was a Phenomenex® Luna® 5μm C18(2) 100 Å 250 x 4.6 mm and was set at 30 ℃. The eluent was a gradient of water/acetonitrile (Table S1) at a flow of 1.00mL/min and a sample injection of 10μL. A diode array detector was used to quantify the *p*-coumaric acid and ferulic acid at a wavelength of 325 nm wavelengths. Two-dimensional heteronuclear single quantum coherence (HSQC) NMR spectroscopy was used to analyse black liquor samples. The black liquor sample was neutralized with HCl and then freeze-dried (9.8-114 mg) and dissolved in deuterium oxide (D_2O, 0.5 mL). HSQC NMR analysis was performed at 25°C on a Bruker 400 MHz spectrometer, a BBO probe with Z gradient. Spectra were acquired with 2048 points and a sweep width of 15ppm in the F2 (1H) dimension and 1024 points and SW=210 ppm in the F1 (13C) dimension. A pulse delay time was 1.0 s, and the acquisition time was 213 msec for proton and 5.7 msec for carbon. TSP was used as an internal reference. Peak assignment was conducted according to previous literature[30-33].

The removal parameter is calculated based on the initial and final value as:

$$Removal = \frac{Initial - Final}{Initial} \times 100\%$$

The recovery percentage of a constituent is calculated based from the recovered mass and removed mass as:

$$Recovery = \frac{Recovered}{removed} \times 100\%$$

Considering mass balance, except the parts left in the outlet and recovered in the recovery solution, there were also unaccounted constituents during the treatment process. This loss is calculated as:

$$Loss = \frac{Initial - fianl - recovered}{Initial} \times 100\%$$

3 Results and discussion

3.1 COD, conductivity and pH changes in the MBRC

Fig. 2 shows time-course changes of COD, conductivity and pH of black liquor and recovery solution in either serial- or parallel-loop operation. Overall, the solution COD decreased significantly in both modes, indicating good treatment performance, and the conductivity drop in the anode and cathode chambers as well as its increase in the recovery chamber suggests an effective ion migration and recovery (Fig. 2A, 2C).

In the case of serial-loop mode, COD concentration of black liquor decreased by 60.8%, from an average of 20475±696 mg/L to 8033±487 mg/L in one 144-h cycle (Fig. 2A). COD removal for the first 48 h was 45.4±2.4%, accounting for over 2/3 of the total COD removal. Such fast decrease in COD is believed attributed to the organic biodegradation by microbial consortium in the anode chamber. A typical anode reaction using acetate as the substrate can be written as ($CH_3COOH + 2H_2O \rightarrow 8H^+ + 2CO_2 + 8e^-$). Such organic removal is also supported by the high current output during the same period, as the electrons generated from organic degradation were transferred to the anode by the microorganisms and subsequently to the cathode to reduce protons to hydrogen gas (Fig. S3). The COD degradation and current dropped gradually toward the end of operation, which is presumably due to the decrease of the black liquor conductivity and the accumulation of recalcitrant organic matters such as lignin[34]. The current output of MBRC ranged from 10.6 mA to 1.0 mA during the 144-h operation (Fig. S3), along with 125 mL of H_2 production. For conductivity, a decrease from 8130±45 μS/cm to 3900±55 μS/cm (52.0±3.6%) was observed, during which a 42.2±2.3% reduction was obtained within the first 48 h. The high reduction rate of conductivity at the beginning was a result of the high current of the MBRC, because current is the main driving force for the ion migration across membranes [34]. In addition, as a result of ion migration some ionic species migrated to the recovery chamber, leading to a conductivity increase (Fig. 2A). The migrated ions included small organic acids (Ac^-, Lac^- and $Prop^-$) and inorganic ions

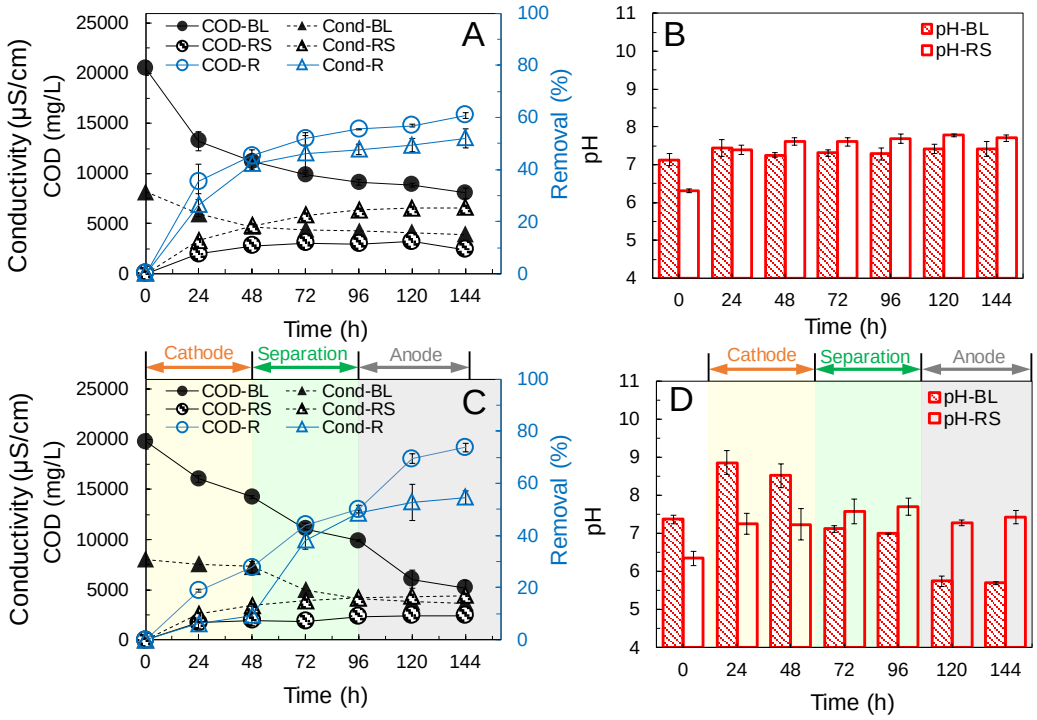

Figure 2. Time-course changes of COD, conductivity, and pH of black liquor (BL) and recovery solution (RS) in different operations. COD and conductivity changes are shown in (A) serial-loop operation and (C) parallel-loop operation. pH changes are shown in (B) serial-loop operation and (D) parallel-loop operation.

(Na^+ and K^+), and the ion transfer and balance are discussed in Fig. 3 and Section 3.2. The pH of the black liquor and the recovery solution varied slightly around 7 (Fig. 2B), and the circulation between the anode and cathode neutralized the H^+ and OH^- generated in the cells [35, 36].

However, lignin removal was not observed because the mild pH change in serial-loop operation. Therefore, we revised the operation strategy to parallel-loop mode, which created a pH gradient that enabled lignin separation and also provided more defined process for elucidating the conversion mechanisms of various components in different MBRC chambers. In this operation, the black liquor was individually and sequentially treated in the cathode chamber, separation chambers, and anode chambers, each for 48 hours (Fig. 2C). Current ranged between 5.8 and 0.9 mA was produced by the MBRC during the 144-h cycle (Fig. S3) with a H_2 yield of 103 mL. The COD concentration in the black liquor decreased stage by stage in each chamber and reached a total removal of 73.8±1.8% during the overall 144-h cycle (Fig. 2C). Approximately 5502±78 mg/L, 4400±235 mg/L, and 4689±432 mg/L COD was removed in the cathode, separation, and anodic stages, respectively. Because the cathode and separation chambers were operated abiotically, the migration of charged organics is believed to be the main removal mechanism (Fig. 3, more discussions in section 3.2). In contrast, organic biodegradation and lignin precipitation could better explain the COD removal in the anode chamber. The conductivity of the liquor decreased from 8040±15 μS/cm to 3650±45 μS/cm (54.6±2.5% drop), which could be attributed primarily to ion migration driven by the bioelectrochemical current. The separation stage contributed to ~70% of the ion removal measured by conductivity due to thin and multiple channels in the membrane stack. As a result of the reduction of COD and conductivity in the black liquor, increases in both COD and conductivity were observed in the recovery solution, which confirms migration of ions from black liquor to the recovery solution across membranes[23]. Ac^- and Na^+ were the main ionic species accumulating in the recovery solution.

Different from the serial-loop mode, the variation of black liquor pH in different chambers in the parallel-loop mode enabled tailored removal and recovery. Due to the continuous accumulation of OH^- from H_2 production in the cathode chamber, the pH of catholyte increased from 7.4±0.1 to 8.9±0.3 in the first 24 h (Fig. 2D). Such alkalization caused the precipitation of Ca^{2+} and Mg^{2+} and resulted in the removal and recovery of these ions from the black liquor. When black liquor entered the separation chamber, the black liquor electrolyte pH dropped from 8.5±0.3 to 7.0±0.02, while the recovery solution pH increased from 7.2±0.4 to 7.7±0.2. This is attributed to the OH^- migration from black liquor to the recovery solution. The pH of black liquor further decreased to 5.7±0.2 after it transferred from the separation chamber to the anode chamber for 48 h. This is due to the generation of H^+ during biological organic degradation in the anode chamber[37, 38]. Electrons were transferred to the anode by the electroactive bacteria, while H^+ was accumulated that led to pH drop and enabled lignin precipitation[39-41]. As the parallel-loop mode showed highly effective treatment of black liquor and efficient separation and recovery of ionic chemicals and biomass, further investigations were focused on the parallel-loop mode.

3.2 Charge transfer and balance in the MBRC

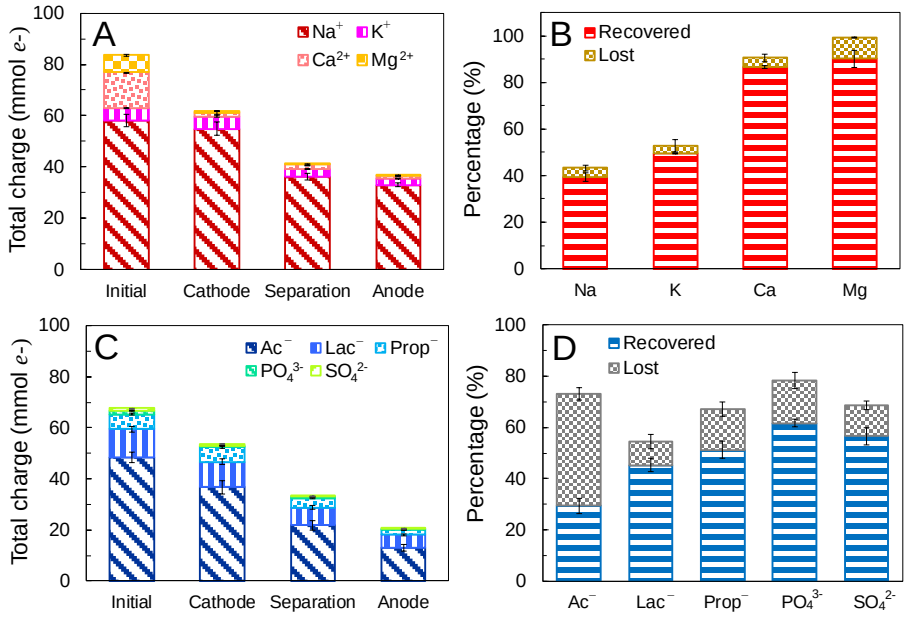

Figure 3. (A) Removals of major cations in different chambers; (B) Total recoveries and losses of cations; (C) Removals of major anions in different chambers; (D) Total losses and recoveries of anions.

Detailed analyses on charge balance during parallel-loop operation were carried out to understand the charge transfer in MBRC. The cations in the black liquor decreased along the whole treatment process (Fig. 3A), but the majority of the cations were removed from black liquor in the cathode chamber. The charge carried by Ca^{2+} and Mg^{2+} reduced by 12.3±0.3 (89.4±0.6%) and 6.0±0.2 (90.8±3.6%) mmol, respectively, which together accounted for over 80% of the charges removed in the cathode chamber (21.8±0.3 mmol). This is believed due to the precipitation of these cations in the form of $Ca(OH)_2$ and $Mg(OH)_2$ in the alkaline environment (Fig. 2D). Such precipitation can be easily separated and recovered from solution using physical method like filtration. Besides Ca^{2+} and Mg^{2+}, 3.2±0.7 mmol of Na^+ and 0.3±0.1 mmol of K^+ were also removed via migration toward the recovery solution.

In the separation stage that received the cathode effluent, a total 20.8±2.9 mmol positive charges were removed from the black liquor, and 98.1% of the removed cations in this stage were Na^+ (18.7±1.7 mmol) and K^+ (1.7±0.2 mmol). The stacked separation chambers played an important role to enable such high removal, as it enabled a multiplied charge transfer efficiency, where the migration of two pairs of cation and ions could be driven by one electron passing through the external circuit[42-44]. In the anode chamber that received the separation chamber effluent, another 4.3±1.4 mmol *e-* was removed from the black liquor, in which the majority was still Na^+ (3.2±1.2 mmol) and K^+ (0.7±0.05 mmol).

Overall, approximately 56.1% of the total cations were removed from the raw black liquor, which included 43.3% of Na^+, 52.7% of K^+, 90.6% of Ca^{2+} and 90.8% of Mg^{2+}. More impressively, 92.2±1.6% of the removed ions were recovered in the recovery solution or as precipitates (Fig. 3B). The removal of ions could be further improved by inserting more pairs of ion exchange membranes to enhance the current efficiency or optimizing the hydraulic retention time in the separation chambers[23]. Beside the mass left in the black liquor effluent and recovered in the recovery solution, 4.0% of Na^+, 3.2% of K^+, 4.0% of Ca^{2+} and 9.1% of Mg^{2+} were lost during the whole treatment process, presumably mainly due to adsorption by electrode and membrane or uptake by the microbe.

The anion removal was also efficient (Fig. 3C). For example, 13.8±2.2 mmol of negative charges carried by anions were removed in the cathode chamber. Among the removed anions, approximately 91.5% was acetate, while small amounts of lactate, propionate, phosphate, and sulfate ions were also removed from black liquor. The separation chamber removed 20.4±1.3 mmol of negatively charged ions via cross-membrane migration. This included 14.9±0.6 mmol of Ac^-, 3.1±0.4 mmol of Lac^-, 2.0±0.1 mmol of $Prop^-$, 0.1±0.1 mmol of PO_4^{3-} and 0.3±0.1 mmol of SO_4^{2-}. The electric potential inside MBRC provided the driving force for all the migration of ionic substances in the separation chamber. Small ions were more readily transferred from the black liquor electrolyte to recovery solution, but larger compounds such as charged lignin species couldn't be removed using this approach[45]. The UV test results proved this, as no lignin content was detected in the recovery solution.

The anode operation removed another 12.8±1.4 mmol of negative charged ions from the separation chamber effluent. This included 8.7±1.3 mmol of Ac^-, 1.9±0.3 mmol of Lac^- and 1.9±0.4 mmol of $Prop^-$. The anode anion removal could be largely attributed to microbial degradation of organics, because such ions couldn't move back to the separation chamber due to the blockage by the CEM. Different from high recovery efficiency of the cations, only 40.4±2.4% of the removed Ac^- was collected in the recovery solution, while 43.5% was lost (Fig. 3D). Such lost mass is believed mainly due to microbial oxidation, which is evidenced by microbial growth in the anode

chamber and sustained current generated during operation. Inorganic anions like phosphate and sulfate were removed by 78.2±4.1% and 68.6±2.3%, respectively, of which 78.9±3.2% of the phosphate and 82.6±1.7% of the sulfate were collected in the recovery solution. The loss of phosphate (16.5%) and sulfate (11.9%) were presumed mainly via bio-uptake or adsorption. Figure S4 shows a process flow diagram to help understand the fate of each constituent in the parallel-loop operation.

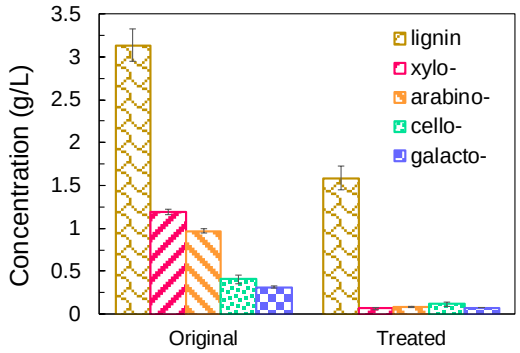

Figure 4. Concentration changes of lignin and oligosaccharides in the black liquor after parallel-loop MBRC treatment. Xylo-: xylo-oligosaccharide; arabio-: arabino-oligosaccharide; cello-: cello-oligosaccharide; galacto-: galacto-oligosaccharide.

3.3 Analysis of lignin and oligosaccharides

The concentrations of lignin, oligomeric xylan, oligomeric arabinan, oligomeric glucan, and oligomer galactan contained in the black liquor were measured using HPLC (Fig. 4). 3.1±0.2 g/L Lignin was contained in the original black liquor, while 49.5±1.2% of the lignin was removed after the treatment in the MBRC. Concomitantly, 0.19±0.01 g of precipitate (dried at 45 ℃ for 24 h) was collected at the bottom of the anolyte circulation bottle. Assuming this precipitation was all lignin units, the recovery percentage of lignin would be 61.2±2.7% via the acidification in the anode chamber. As mentioned previously, sulfuric acid is used in commercial practice to precipitate lignin at low pH, which is costly and further increase the salinity of the black liquor[41, 46]. Herein, taking advantage of the acidic nature of the MBRC anode chamber offers a low-cost and an imported energy-free alternative for lignin precipitation and separation. Together with the removal of lignin units, the

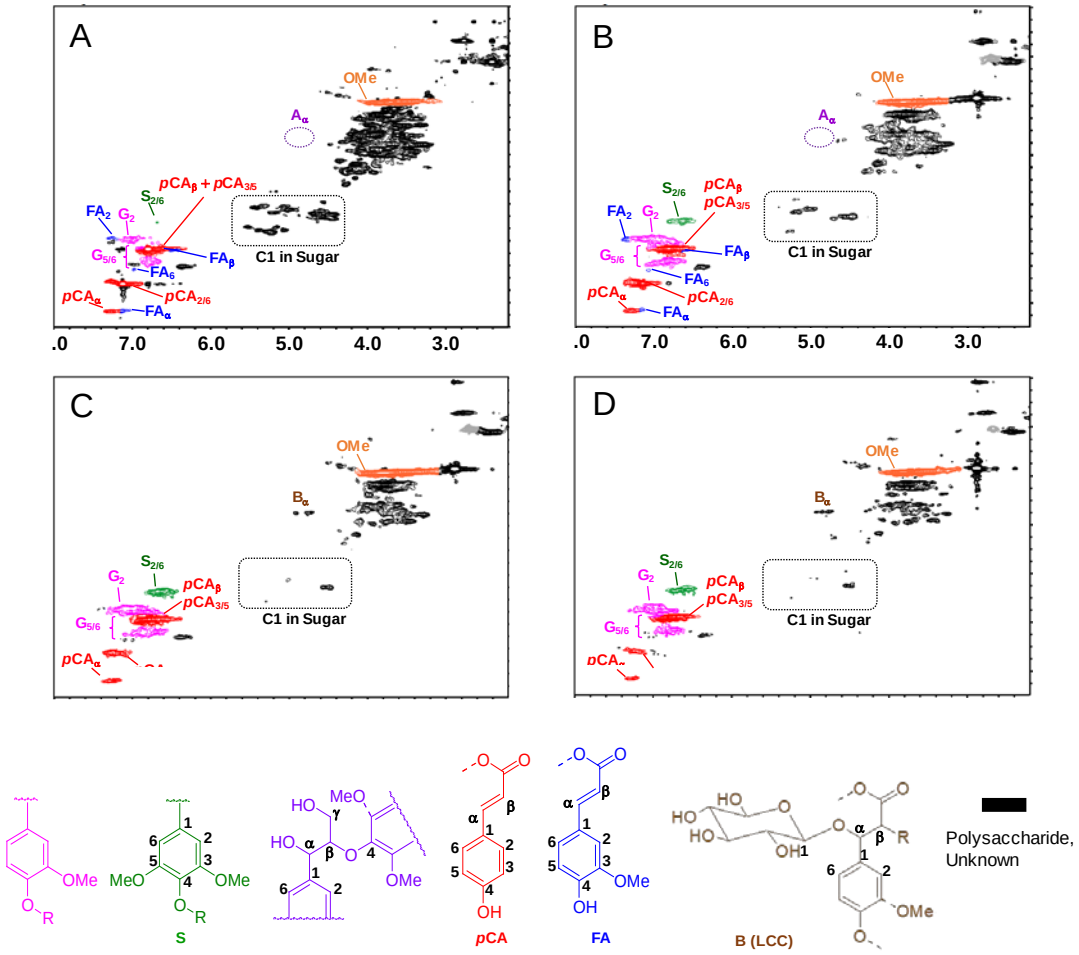

Figure 5. HSQC NMR spectra of the (A) original black liquor, (B)cathodic stage effluent, (C)separation stage effluent, and (D) anodic stage effluent of the MBRC treatment. G: guaiacyl; S: syringyl; A: β-O-4; *p*CA: *p*-coumarate; FA: ferulate; B (LCC): lignin carbohydrate complex.

concentrations of oligosaccharides also decreased significantly in MBRC treatment (Fig. 4). Most of the xylo-oligosaccharides (94.4±1.2%), arabino-oligosaccharides (91.4±1.0%), cello-oligosaccharides (71.6±2.2%), and galacto-oligosaccharides (76.3±1.0%) were removed. Since lignin is always chemically linked with cell wall polysaccharides and thus the transformation or removal of lignin and oligosaccharides are closely related[32].

Two-dimensional HSQC NMR spectroscopy was used to investigate the corresponding changes of lignin and sugar unit structures in the black liquor (Fig. 5). The main signals in the well-resolved aromatic regions (δ_C/δ_H 100-150/6.0-7.2 ppm) of original black liquor spectra corresponded to the aromatic rings of guaiacyl (G) and syringyl (S) lignin units (Fig. 5A). A prominent signal indicating the $S_{2/6}$ lignin units was observed at δ_C/δ_H 107.5/6.68 ppm, along with the strong signal of G_2 at δ_C/δ_H 114.4/6.99 and $G_{5/6}$ at 117.9/6.88 and 123.4/3.78 ppm, respectively. The *p*-coumarates (*p*CA) were assigned at δ_C/δ_H 117-120.8/6.3-6.96 ppm for pCA_{2} and $pCA_{3/5}$, at δ_C/δ_H 132.5/7.12 ppm for $pCA_{2/6}$, and at δ_C/δ_H 143.7/7.3 ppm as $pCA_{}$. Meanwhile, signals of ferulates (FA) were also observed as indicated by the FA_2 (δ_C/δ_H 114.0/7.29 ppm), $FA_{}$ (δ_C/δ_H 119.0/6.50 ppm), FA_6 (δ_C/δ_H 126.4/6.97 ppm), and $FA_{}$ (δ_C/δ_H 143.4/7.12 ppm) peaks. Other than aromatic structures, the original black liquor also contained large amount of carbohydrates, indicated by the circled anomeric C1 peaks in oligosaccharides at region δ_C/δ_H 98-114/4.3-5.6 ppm. Verified by the HPLC test, 1.19±0.03 g/L xylo-oligosaccharide, 0.97±0.03 g/L arabino-oligosaccharide, 0.41±0.05 g/L cello-oligosaccharide, and 0.31±0.01 g/L galacto-oligosaccharide were contained in the original black liquor (Fig. 4). The HSQC NMR spectrum of the cathodic stage effluent is similar as that of the original black liquor, where the prominent signals of G, S, *p*CA and FA were all distinguished (Fig. 5B). The spectra of separation stage effluent and anodic stage effluent show different compositions than the original and cathodic black liquor (Fig. 5C&D), where the FA peaks represent disappearing ferulate units. Interestingly, a correlation peak at δ_C/δ_H 74.7/4.89 ppm in the separation and anodic stage effluents appeared at similar chemical shifts to that of C_α-H_{α} in β-*O*-4 aryl ether unit, while no A_{α} correlation peak was observed in original black liquor and cathodic stage effluent. A possible explanation is that the hydroxy group in carbohydrate at the anomeric position (C1 position) was added to C_α in soluble *p*-coumaric acid and ferulic acid sodium salt during the cathodic electrochemical reaction, which generated benzyl ether type lignin-carbohydrate complexs (LCCs). The correlation peak of C_α-H_α in the LCC appear at the similar chemical shift of A_α in the β-*O*-4 unit[32]. These LCCs were precipitated because of low solubility in the reduced pH conditions in the separation and anode chambers[32]. This is supported by HPLC results, which show low coumaric and ferulate acid in the separation effluent and anolyte. Concomitantly, the C1 sugar signal of the separation and anode effluents were much weaker than in the previous two spectra.

3.4 System Features and Outlook

Black liquor is a complex and recalcitrant feedstock for traditional biological treatment, and by taking advantage of the synergy between biodegradation and the self-generated electrical field and pH gradient, the MBRC approach offers a tailored approach and good performance in removing different dilute constituents and recovering value-added products (Fig. S4). Low pH in the anode and high pH in the cathode chambers have been a main challenge in microbial electrochemical systems, and traditionally large amount buffer solution or high-energy recirculation are needed to neutralize the electrolyte. In this MBRC process, we rather took advantage of this pH gradient by utilizing the low pH in the anode to enable the precipitation and separation of recalcitrant lignin and LCCs, and the high pH in the cathode chamber allowed the precipitation of Ca^{2+}, Mg^{2+} and other ions associated with hardness. In the meantime, under the self-generated electrical potential between the anode and the cathode, charged organic and inorganic ion species such as Na^+ and Ac^- were efficiently transferred from the black liquor to the recovery chambers, and for major ions the recovery efficiency was higher than 90%. Overall, these complementary removal and recovery mechanisms make MBRC a unique process for black liquor treatment and valorization.

This study shows the proof-of-concept that value-added products can be recovered during black liquor treatment using microbial electrochemical processes, and the recovered products like organic acids, salts, and biomass have higher economic values than the energy generated from traditional gasification. Moreover, the high efficiency and low energy operation makes the MBRC promising for further research and development. Groups have scaled microbial electrochemical systems from lab scale to pilot scales and demonstrated their long-term operation using real wastewater streams[47, 48]. Such scale-up experience can be good references for MBRC development. To advance the technology, there are still many challenges to be addressed in future research. The level of degradation needs to be further enhanced, and major tasks should focus on breaking down of lignocellulosic fibers to enhance biodegradability and ion and electron transfers. More developments are needed for the separation of precipitated lignin and salts in the anode and cathode chambers, anti-scaling and anti-fouling measures are needed for system development. More understandings are also needed to decipher the transformation mechanisms of different ion species and lignin and oligosaccharides.

Conflicts of interest

There are no conflicts to declare.

Acknowledgements

We appreciate the financial support from U.S. Department of Energy (DOE) and University of Colorado Boulder Technology Transfer Office. This work was authored by Alliance for Sustainable Energy LLC, the manager and operator of the National Renewable Energy Laboratory for DOE under Contract No. DE-AC36-08GO28308. Funding provided by U.S. Department of Energy Office of Energy Efficiency and Renewable Energy Solar Energy Technologies Office. The views expressed in the article do not necessarily represent the views of the DOE or the U.S. Government. The U.S. Government retains and the publisher, by accepting the article for

Notes and references

1. A. J. Ragauskas, G. T. Beckham, M. J. Biddy, R. Chandra, F. Chen, M. F. Davis, B. H. Davison, R. A. Dixon, P. Gilna, M. Keller, P. Langan, A. K. Naskar, J. N. Saddler, T. J. Tschaplinski, G. A. Tuskan and C. E. Wyman, *Science*, 2014, **344**.
2. V. Menon and M. Rao, *Prog. Energy Combust. Sci.*, 2012, **38**, 522-550.
3. Y. Qian, Y. Deng, X. Qiu, H. Li and D. Yang, *Green Chemistry*, 2014, **16**, 2156-2163.
4. S. Gillet, M. Aguedo, L. Petitjean, A. R. C. Morais, A. M. da Costa Lopes, R. M. Łukasik and P. T. Anastas, *Green Chemistry*, 2017, **19**, 4200-4233.
5. M. Naqvi, J. Yan and E. Dahlquist, *Bioresour. Technol.*, 2010, **101**, 8001-8015.
6. X. Chen, E. Kuhn, E. W. Jennings, R. Nelson, L. Tao, M. Zhang and M. P. Tucker, *Energy & Environmental Science*, 2016, **9**, 1237-1245.
7. X. Chen, W. Wang, P. Ciesielski, O. Trass, S. Park, L. Tao and M. P. Tucker, *ACS Sustainable Chemistry & Engineering*, 2016, **4**, 324-333.
8. X. Chen, E. Kuhn, N. Nagle, R. Nelson, L. Tao, N. Crawford and M. Tucker, *Frontiers in Energy Research*, 2018, **6**.
9. R. Davis, L. Tao, C. Scarlata, E. C. D. Tan, J. Ross, J. Lukas and D. Sexton, *Process Design and Economics for the Conversion of Lignocellulosic Biomass to Hydrocarbons: Dilute-Acid and Enzymatic Deconstruction of Biomass to Sugars and Catalytic Conversion of Sugars to Hydrocarbons*, United States, 2015.
10. A. Pérezgimeno, J. Navarropedreño, M. B. Almendrocandel, I. Gómez and M. M. Jordán, *Journal of Soils & Sediments*, 2015, **16**, 1-10.
11. H. Wang, H. Luo, P. H. Fallgren, J. Song and Z. J. Ren, *Biotechnol. Adv.*, 2015, **33**, 317-334.
12. P. L. McCarty, J. Bae and J. Kim, *Environ. Sci. Technol.*, 2011, **45**, 7100-7106.
13. R. Shen, Y. Jiang, Z. Ge, J. Lu, Y. Zhang, Z. Liu and Z. J. Ren, *Applied Energy*, 2018, **212**, 509-515.
14. L. Lu and Z. J. Ren, *Bioresour. Technol.*, 2016, **215**, 254-264.
15. A. Gálvez, J. Greenman and I. Ieropoulos, *Bioresour. Technol.*, 2009, **100**, 5085-5091.
16. D. Call and B. E. Logan, *Environ. Sci. Technol.*, 2008, **42**, 3401-3406.
17. B. E. Logan and K. Rabaey, *Science*, 2012, **337**, 686-690.
18. H. Luo, P. E. Jenkins and Z. Ren, *Environ. Sci. Technol.*, 2011, **45**, 340-344.
19. X. Chen, D. Sun, X. Zhang, P. Liang and X. Huang, *Sci. Rep.*, 2015, **5**.
20. M. Qin, Y. Liu, S. Luo, R. Qiao and Z. He, *Chem. Eng. J.*, 2017, **327**, 924-931.
21. X. Chen, P. Liang, X. Zhang and X. Huang, *Bioresour. Technol.*, 2016, **215**, 274-284.
22. K. Zuo, Z. Wang, X. Chen, X. Zhang, J. Zuo, P. Liang and X. Huang, *Environ. Sci. Technol.*, 2016, **50**, 7254-7262.
23. X. Chen, H. Zhou, K. Zuo, Y. Zhou, Q. Wang, D. Sun, Y. Gao, P. Liang, X. Zhang, Z. J. Ren and X. Huang, *Chem. Eng. J.*, 2017, **330**, 692-697.
24. Y. Gao, D. Sun, H. Wang, L. Lu, H. Ma, L. Wang, Z. J. Ren, P. Liang, X. Zhang, X. Chen and X. Huang, *Environmental Science: Water Research & Technology*, 2018, **4**, 1427-1438.
25. R. A. Rozendal, H. V. M. Hamelers and C. J. N. Buisman, *Environ. Sci. Technol.*, 2006, **40**, 5206-5211.
26. L. Lu, D. Hou, Y. Fang, Y. Huang and Z. J. Ren, *Electrochim. Acta*, 2016, **206**, 381-387.
27. D. Hou, L. Lu and Z. J. Ren, *Water Res.*, 2016, **98**, 183-189.
28. X. Chen, Y. Gao, D. Hou, H. Ma, L. Lu, D. Sun, X. Zhang, P. Liang, X. Huang and Z. J. Ren, *Environmental Science & Technology Letters*, 2017, **4**, 305-310.
29. M. Alaraj, Z. J. Ren and J.-D. Park, *J. Power Sources*, 2014, **247**, 636-642.
30. H. Kim, J. Ralph and T. Akiyama, *Bioenergy Research*, 2010, **8**, 576-591.
31. S. D. Mansfield, H. Kim, F. Lu and J. Ralph, *Nature Protocols*, 2012, **7**, 1579.
32. T.-Q. Yuan, S.-N. Sun, F. Xu and R.-C. Sun, *J. Agric. Food. Chem.*, 2011, **59**, 10604-10614.
33. L. da Costa Sousa, M. Jin, S. P. S. Chundawat, V. Bokade, X. Tang, A. Azarpira, F. Lu, U. Avci, J. Humpula, N. Uppugundla, C. Gunawan, S. Pattathil, A. M. Cheh, N. Kothari, R. Kumar, J. Ralph, M. G. Hahn, C. E. Wyman, S. Singh, B. A. Simmons, B. E. Dale and V. Balan, *Energy & Environmental Science*, 2016, **9**, 1215-1223.
34. X. Chen, H. Sun, P. Liang, X. Zhang and X. Huang, *J. Power Sources*, 2016, **324**, 79-85.
35. Y. Qu, Y. Feng, X. Wang, J. Liu, J. Lv, W. He and B. E. Logan, *Bioresour. Technol.*, 2012, **106**, 89-94.
36. X. Chen, P. Liang, Z. M. Wei, X. Y. Zhang and X. Huang, *Bioresour. Technol.*, 2012, **119**, 88-93.
37. Z. He, Y. Huang, A. K. Manohar and F. Mansfeld, *Bioelectrochemistry*, 2008, **74**, 78-82.
38. H. Luo, P. Xu, T. M. Roane, P. E. Jenkins and Z. Ren, *Bioresour. Technol.*, 2012, **105**, 60-66.
39. A. Garg, I. M. Mishra and S. Chand, *J. Hazard. Mater.*, 2010, **180**, 158-164.
40. T. Q. To, C. Kenny, S. Cheong and L. Aldous, *Green Chemistry*, 2017, **19**, 2129-2134.
41. V. C. Uloth, *Pulp Paper Can*, 1989, **90**.
42. X. Chen, X. Xia, P. Liang, X. X. Cao, H. T. Sun and X. Huang, *Environ. Sci. Technol.*, 2011, **45**, 2465-2470.
43. Z. Ge, C. G. Dosoretz and Z. He, *Desalination*, 2014, **341**, 101-106.
44. Y. Kim and B. E. Logan, *Environ. Sci. Technol.*, 2011, **45**, 5840-5845.
45. M. Haddad, S. Mikhaylin, L. Bazinet, O. Savadogo and J. Paris, *J. Colloid Interface Sci.*, 2017, **488**, 39-47.
46. W. Zhu, G. Westman and H. Theliander, *Chinese Journal of Clinical Hepatology*, 2014, **34**, 77-97.
47. C. Forrestal, A. Haeger, L. Dankovich Iv, T. Y. Cath and Z. J. Ren, *Environmental Science: Water Research & Technology*, 2016, **2**, 353-361.
48. P. Liang, R. Duan, Y. Jiang, X. Zhang, Y. Qiu and X. Huang, *Water Res.*, 2018, **141**, 1-8.

